

Sequence analysis, *in silico* modeling and docking studies of Caffeoyl CoA-*O*-methyltransferase of *Populus trichopora*

Navneet Phogat · Vaibhav Vindal · Vikash Kumar ·
Krishna K. Inampudi · Nirmal K. Prasad

Received: 2 September 2009 / Accepted: 5 January 2010 / Published online: 19 February 2010
© Springer-Verlag 2010

Abstract Caffeoyl coenzyme A-*O*-methyltransferases (CCoAOMTs) which are characterized under class I plant OMTs, methylates CoA thioesters, with an *in vitro* kinetic preference for caffeoyl CoA. CCoAOMTs exhibit association with lignin biosynthesis by showing a prime role in the synthesis of guaiacyl lignin and providing the substrates for synthesis of syringyl lignin. The sequence analysis of CCoAOMT from *Populus trichopora* exhibits 58 nucleotide substitutions, where transitions overcome transversions. Validation of homology models of both CCoAOMT1 and 2 isoforms reveals that 92.4% and 96% residues are falling in the most favorable region respectively in the Ramachandran plot, indicating CCoAOMT2 as the more satisfactory model, and the overall quality factor of both isoforms is 98.174. The structural architecture analysis is showing very good packing of residues similar to protein crystal structures data. The active site residues and substrate-product interactions showed that CCoAOMT2 possesses more affinity toward caffeoyl CoA, feruloyl CoA, 5-hydroxy feruloyl CoA and sinapoyl CoA than CCoAOMT1, therefore it exist in a more active conformation. The affinity of CCoAOMT2 with feruloyl

CoA is highest among all the affinities of both CCoAOMT isoforms with their substrates and products. This information has potential implications to understand the mechanism of CCoAOMT related enzymatic reactions in *Populus trichopora*, however the approach will be applicable in prediction of substrates and engineering 3D structures of other enzymes as well.

Keywords CCoAOMT isoforms · Docking · Homology modeling · Lignin · *Populus trichopora* · Sequence analysis

Introduction

The plant *O*-methyl transferases (OMTs), catalyzing the *O*-methylation process by transferring the methyl group from S-adenosyl methionine (SAM) to the hydroxyl group of an acceptor molecules which are usually hydroxycinnamic acid or its esters, can be divided into two groups indicated as class- I and class- II plant OMTs [1–4]. Class- I plant OMTs, represented by Caffeoyl CoA-*O*-methyltransferases (CCoAOMT) and of molecular weight around 28 KDa. CCoAOMTs are known to methylate coenzyme A (CoA) thioesters including Caffeoyl CoA and 5-hydroxyferuloyl CoA, with an *in vitro* kinetic preference for Caffeoyl CoA, results in formation of cross linked polymer lignin which provides a physical barrier against pathogen infection. The same enzyme also exhibits specificity for products feruloyl CoA and sinapoyl CoA [1, 5–9]. On the other hand, class-II plant OMTs of molecular weight around 40 KDa include two types of enzymes; out of them, Caffeic acid-*O*-methyltransferases (COMTs) exhibit substrate specificity for free acids like caffeic acid and 5-hydroxy ferulic acid, with a preference for 5-hydroxyl compounds and OMTs

N. Phogat · V. Kumar · N. K. Prasad (✉)
Department of Biotechnology, Goa University,
Taleigao Plateau, Goa, India 403206
e-mail: nimmynirmal@gmail.com

V. Vindal
Department of Biotechnology, University of Hyderabad,
Gachibowli, Hyderabad, 500046 India

K. K. Inampudi
Division of Allergy and Infectious Disease, UW medical school,
University of Washington,
Seattle, WA 98195, USA

Table 1 Nucleotide substitution and amino acid change profile in the CCoAOMT isoforms

Nucleotide position	Change	Nucleotide position	Change	Nucleotide position	Change	Amino acid position	Change
7	A/G	8		9		3	T/A
25		26		27	A/G		
28		29	G/C	30	C/T	10	S/T
34		35		36	A/C		
43		44		45	C/T		
46		47		48	G/A		
100		101		102	C/T		
106		107		108	T/C		
115		116		117	T/C		
145		146		147	C/T		
148		149		150	G/A		
154	G/T	155		156		52	V/L
214		215		216	T/C		
223		224		225	G/A		
232	G/A	233		234		78	V/I
241		242		243	A/G		
256		257		258	C/T		
265		266	A/T	267		89	V/F
292		293		294	C/T		
295		296		297	G/T		
313		314		315	C/A		
355	T/C	356		357			
364		365		366	A/G		
367		368		369	A/G		
385	G/C	386		387	T/G	129	V/L
388		389	C/A	390	G/A	130	A/E
400		401		402	T/G	134	D/E
421		422		423	A/G		
430		431		432	T/C		
451		452		453	G/A		
457		458	G/A	459		153	C/Y
466		467	G/C	468		156	S/T
469		470	T/A	471		157	F/Y
472		473		474	T/C		
508		509		510	A/T		
511		512		513	T/C		
514		515		516	T/C		
538		539		540	A/C		
544		545		546	T/C		
547		548		549	T/A		
553	C/T	554		555			
562		563		564	C/T		
571		572		573	T/C		
595		596		597	T/A		
601	C/G	602		603	T/C	201	P/A
607		608		609	A/G		
610		611		612	A/G		
634		635		636	C/T		
649	T/C	650		651			

Table 1 (continued)

Nucleotide position	Change	Nucleotide position	Change	Nucleotide position	Change	Amino acid position	Change
658		659		660	C/T		
670		671		672	T/A		
715		716		717	C/T		
739	C/A	740		741	A/G	247	Q/K

while other OMTs include OMTs causing methylation of flavonoids, alkaloids and other secondary metabolites [1, 5, 6, 9]. A new class of OMTs has been demonstrated, which includes enzymes of low molecular weight and are known to exhibit substrate specificities for caffeoyl CoA and flavonoids and are being used for regioselective synthesis of flavonoids and other chemicals [1, 10–14].

The CCoAOMTs has been characterized from a number of plants, including Poplar (*Populus spp.*) [15], Pine (*Pinus taeda*) [16], Tobacco (*Nicotiana tabacum*) [17], Alfalfa (*Medicago sativa*) [18], Zinnia (*Zinnia elegans*) [19], Carrot (*Daucus carota*) [20] and Parsley (*Petroselinum crispum*) [21]. It is very critical for lignifying tissues, explained on the basis of immunolocalization and tissue printing studies [22]. The CCoAOMTs cannot act on free caffeic acid; CoA becomes very essential moiety for the enzyme's activity [8, 23, 24]. CCoAOMT contains a well ordered active site, having characteristic divalent metal (Ca^{+2}) binding site suggests a metal dependent catalytic mechanism [2, 5, 25]. The Ca^{+2} , playing an important role in transmethylation process and causing the deprotonation of 3-hydroxyl of caffeoyl CoA, leads to the formation of oxyanion which is in close proximity to methyl group of SAM (S-adenosylmethionine), facilitating transmethylation [5]. CCoAOMT exist in dimeric form which is not critical for substrate recognition and transmethylation. Substrates and cofactors are known to interact with monomer only, while other OMTs of the plant dimeric form plays an important role in substrate recognition [5, 26, 27]. Plant CCoAOMTs are related to mammalian catechol OMTs in structural, functional and evolutionary parameters, explained on the basis of similarity in substrate binding site and utilization of a divalent cation in the catalytic mechanism. However different oligomerization states are present with catechol OMTs [5]. The crystal structure of alfalfa CCoAOMT is already being studied and the structural information is being applied to study the substrate preferences of CCoAOMTs of other plants [5]. The present study deals with the analysis of CCoAOMT gene from a model plant *Populus trichopora*, a plant which is economically important for producing high quality paper and plywood. It reports the comparative sequence analysis, homology modeling and docking studies of the enzyme caffeoyl CoA-*O*-methyltransferase of *Populus trichopora*.

Methods

Sequence analysis

Gene sequences encoding Caffeoyl CoA-*O*-methyltransferases (CCoAOMTs) of *Populus trichopora* (GenBank Accession numbers: XM_002313089 and XM_002298693) were selected. Homologous gene sequences were retrieved by using 'BLASTN' against non-redundant database of NCBI. All the duplicate entries as well as partial sequences were removed for the analysis. Multiple sequence alignment of *Populus trichopora* CCoAOMT genes was analyzed to map the sequence conservation and variation in all sequences. Amino acid conservation and substrate binding motifs were mapped in translated sequences. Conserved sequence positions in *Populus trichopora* protein were identified in the multiple sequence alignment.

Molecular modeling of CCoAOMT

The 3D structures of both the isoforms of CCoAOMT were constructed using MODELLER 9v7 [28, 29]. Alfalfa CCoAOMT, PDB accession numbers: 1SUS.pdb and 1SUI.pdb were chosen as templates for molecular modeling. Coordinates from the reference protein (1SUS and 1SUI) to the structurally conserved regions (SCRs), structurally variable regions (SVRs), N-termini and C-termini were assigned to the target sequence based on the satisfaction of spatial restraints. All side chains of the model protein were set by rotamers. The obtained structures from the Modeller were evaluated for its stereochemical quality by using PROCHEK [30] and environment profile using ERRAT graph [31].

Molecular dynamics simulations

3D structure refinement of CCoAOMT were carried out using energy minimization and molecular dynamics. It was performed using VEGA ZZ [32], Nano Molecular Dynamics (NAMD 2.6) [33] and Chemistry of Harvard Molecular Modelling (CHARMM22) force field and charges for proteins [34, 35]. The simulations and energy minimization were carried out in 60,000 step minimization of the designed side chains and solvent to remove bad contacts. Minimum switching distance of 8.0 Å and a cut off of 12.0

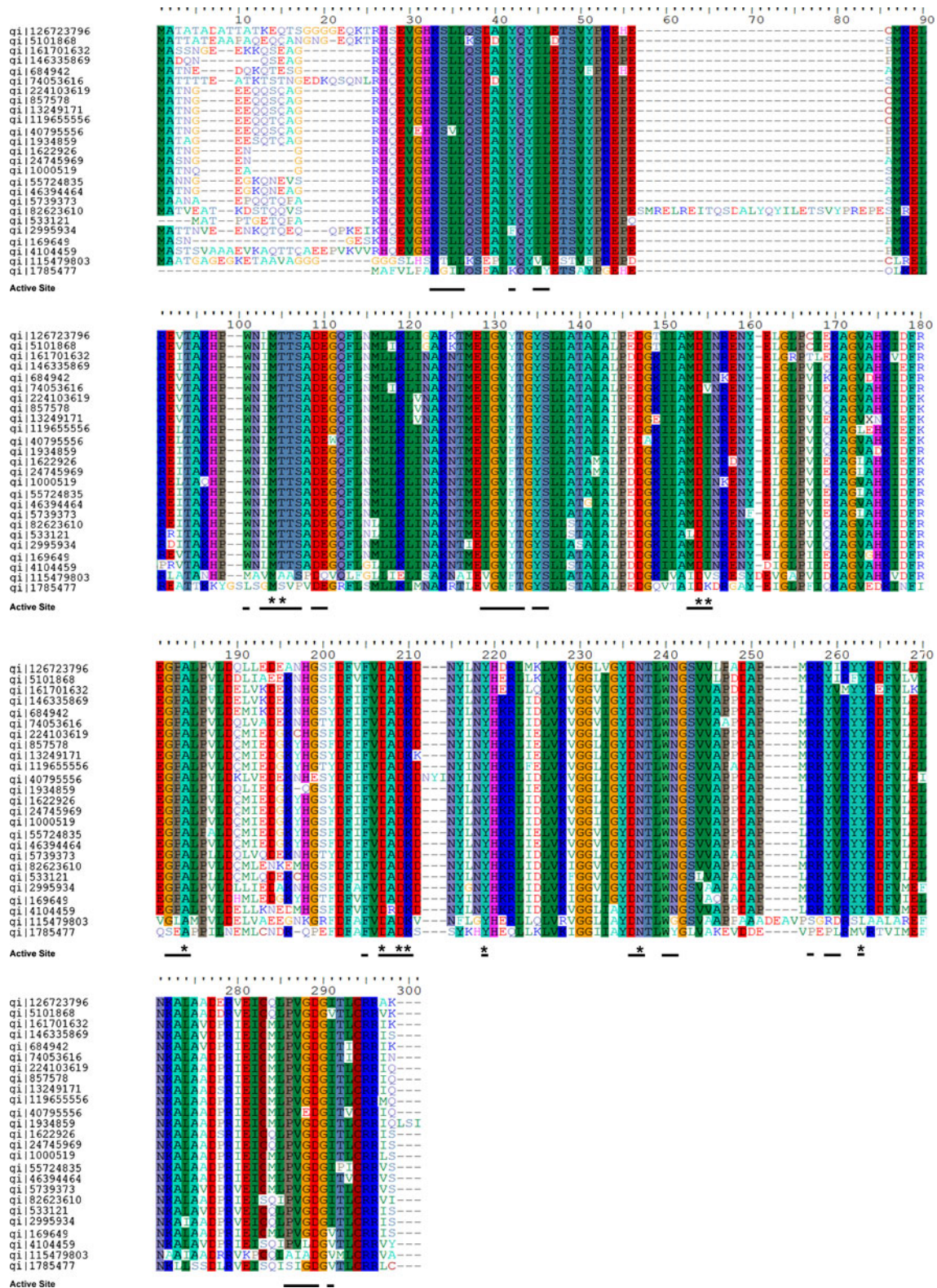


Fig. 1 Multiple sequence alignments of CCoAOMT homologues showing conserved regions, where ‘—’ represents active site residues, and ‘*’ represents interacting active site residues of *P. trichopora* CCoAOMT isoforms

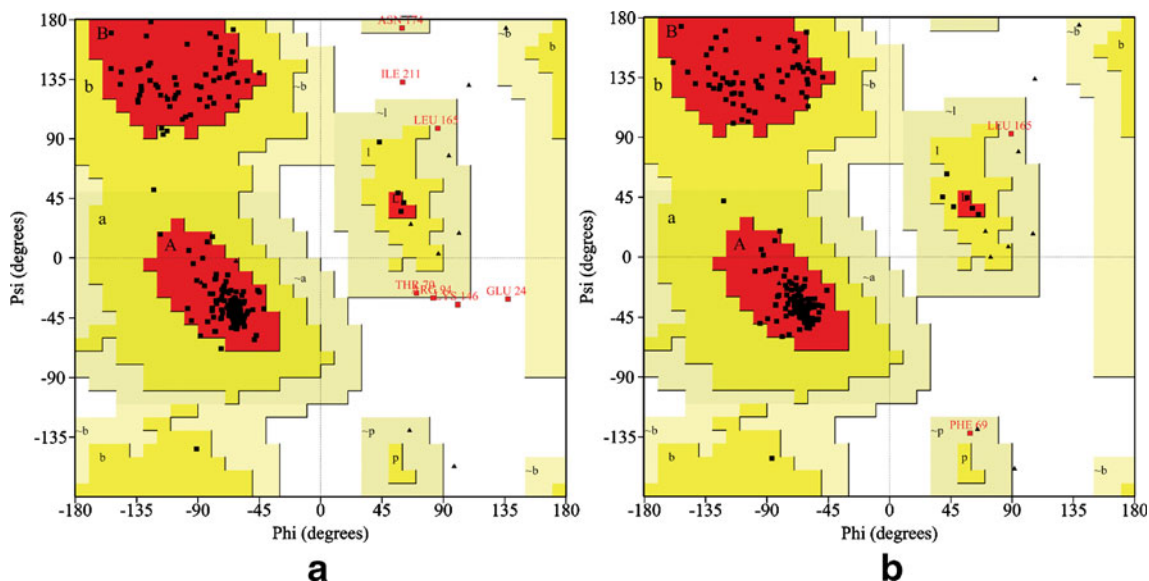


Fig. 2 Residue profile of CCoAOMT1 (a) and CCoAOMT2 (b) isoforms in Ramachandran's plot

Å for Vander Walls interactions was used, pair list of the non-bonded interactions was recalculated every 20 steps with a pair list distance of 13.5 Å. The resultant energy minimized protein models were used for the active site identification and for docking with substrates.

Structural and packing architecture of the models

Mean hydrogen bonds distances and mean dihedral angles of the energy minimized structures were calculated. Accessible surface area of the structures and packing volume were analyzed by VADAR 1.4 [36]. The obtained statistics were analyzed for the homology modeled structures quality. PROCHECK and ERRAT graph analysis were done again to check the residues falling in the most favored region in the Ramachandran plot and overall quality factor of the models.

Docking studies

Preparation of the target and substrates for docking

The binding pockets and active sites of CCoAOMTs were identified by Computed Atlas of Surface Topography of

Proteins (CASTp) program [37]. Conserved substrate binding motifs and the active residues were identified in the predicted binding pockets by motifs similarity profile. The substrate molecules were obtained from Pubchem database of NCBI [38], and all the substrate molecules used for docking were converted in 3D with VEGA ZZ software. Molecules were docked to the binding sites by CCDC's GOLD 3.2 (Genetic Optimization for Ligand Docking, <http://www.ccdc.cam.ac.uk>) [39]. The binding region for the docking study was defined as a 10 Å radius sphere centered on the active site. One-hundred genetic

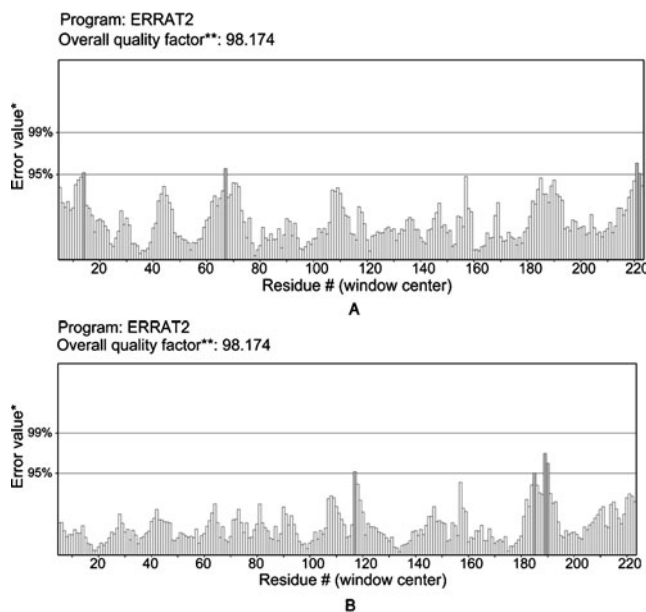


Fig. 3 CCoAOMT1 (a) and CCoAOMT2 (b) residue environmental profile validated by ERRAT2 program

Table 2 Ramachandran plot statistics of CCoAOMT isoforms

Statistics	CCoAOMT1	CCoAOMT2
Residues in most favored region	92.4%	96.0%
Residues in additionally allowed region	4.0%	3.0%
Residues in generously allowed region	1.5%	1.0%
Residues in disallowed region	2.0%	0.0%

Table 3 Structural characteristics and features of the models

Isoform	MHBD(Å)	MHBE	MHP _h	MHP _s	MCG ⁺	MCG ⁻	MRV (Å ³)	TV (Å ³)
CCoAOMT 1	2.3	-1.5	-64.3	-39.9	-64.5	63.2	137.1	31131.6
CCoAOMT 2	2.2	-1.6	-64.5	-39.1	-68.0	62.9	136.9	31074.6

MHBD - Mean hbond distance; MHBE - Mean hbond energy; MHP_h - Mean Helix Phi; MHP_s - Mean Helix Psi; MCG⁺ - Mean Chi Gauche+; MCG⁻ - Mean Chi Gauche-; MRV - Mean residue volume; TV - Total volume (packing)

algorithm (GA) runs were performed for each compound, and 10 ligand bumps were allowed in an attempt to account for mutual ligand/target fit. For each of the GA run a maximum number of 100,000 operations were performed on a population of 100 individuals with a selection pressure of 1.1. The number of islands was set to 5 with a niche size of 2. The weights of crossover, mutation, and migration were set to 95, 95, and 10 respectively. The scoring

function GoldScore implemented in GOLD was used to rank the docking positions of the molecules, which were clustered together when differing by more than 2 Å in rmsd. The best ranking clusters for each of the molecules were selected.

Enzyme-substrate interactions

All the interactions were visually inspected in CCDc's SILVER 1.1.1 software (<http://www.ccdc.cam.ac.uk>). Hydrogen bonds within the 10 Å radius interaction space of active site and close contacts with the substrate atoms were analyzed.

Results

Conservation and variation in the sequences

The aligned sequences of CCoAOMT isoforms contain 58 base pair substitutions in 744 base pairs (7.79% of the nucleotide positions); there are no insertions or deletions. Nucleotide transitions (A/G and C/T=38) greatly outnumber transversions (A/T, A/C, G/C and G/T=20). Third positions in codons were the most variable (74.1%) followed by first positions (15.5%) and only six changes were observed in second positions, which are responsible of only 13 amino acid residues difference in the protein sequence. Table 1 describes detailed information of the nucleotide substitutions and amino acid changes in the sequence. The multiple sequence alignment of homologous CCoAOMT protein sequences of 25 different plants including *Populus trichopora* sequence are shown in Fig. 1. It clearly showed the highly conserved motifs of homologous CCoAOMT protein sequences and comparison of active site residues which are participating in the protein substrate/product interactions.

Structural quality of homology models

For both the isoforms (CCoAOMT1 and CCoAOMT2) out of 10 structures generated by the MODELLER 9v7, the one with the lowest value of the MODELLER objective function was selected as the best model for CCoAOMT1 and



Fig. 4 Catalytic active sites of CCoAOMT1 (a) and CCoAOMT2 (b) predicted by CASTp calculations, green colored region in the model represents the active site cavity

CCoAOMT2. The first 20 residues are producing random coils in both models, and were deleted from the structures. These models were further refined by energy minimization and molecular dynamics. The central core protein region is forming Rossman fold which plays a very important role in conformational change of the protein. This central core region mainly consists of β sheets surrounded by helices. The structural geometry of the models were checked by Ramachandran plot computed by PROCHECK program, before energy minimization and molecular dynamics the models show the backbone ϕ and ψ dihedral angles of CCoAOMT1 and CCoAOMT2 are 91.4% and 94.5% residues are located in the most favorable regions respectively, the refined models show 92.4% of CCoAOMT1 and 96.0% of CCoAOMT2 residues are located in the most favorable regions in the Ramachandran plot (Fig. 2a and b). All the Ramachandran's plot statistics are documented in Table 2. The overall quality factor is 98.174 for both enzyme isoforms (Fig. 3a and b), which indicates very good residues environmental profile of the modeled enzymes.

Models packing architecture

In addition to mean helix phy, psi parameters and mean Chi Gauche values, mean hydrogen bond distances and energy in the models were similar to the known protein crystal structures data. The CCoAOMT1 and 2 mean residue volume were 137.1 \AA^3 and 136.9 \AA^3 respectively, which shows very good packing. The whole CCoAOMT 1 and 2 models having 31131.6 \AA^3 and 31074.6 \AA^3 total packing volume respectively; all the structural parameters are recorded in Table 3.

Catalytic active site identification of CCoAOMT1 and 2 isoforms

The binding sites of CCoAOMT1 and CCoAOMT2 were searched based on the CASTp calculation server. In the present study, locating the cavity sites in the CCoAOMT1 and 2 structures and the largest cavity site displayed on the structure is selected as active site shown in Fig. 4a and b. It

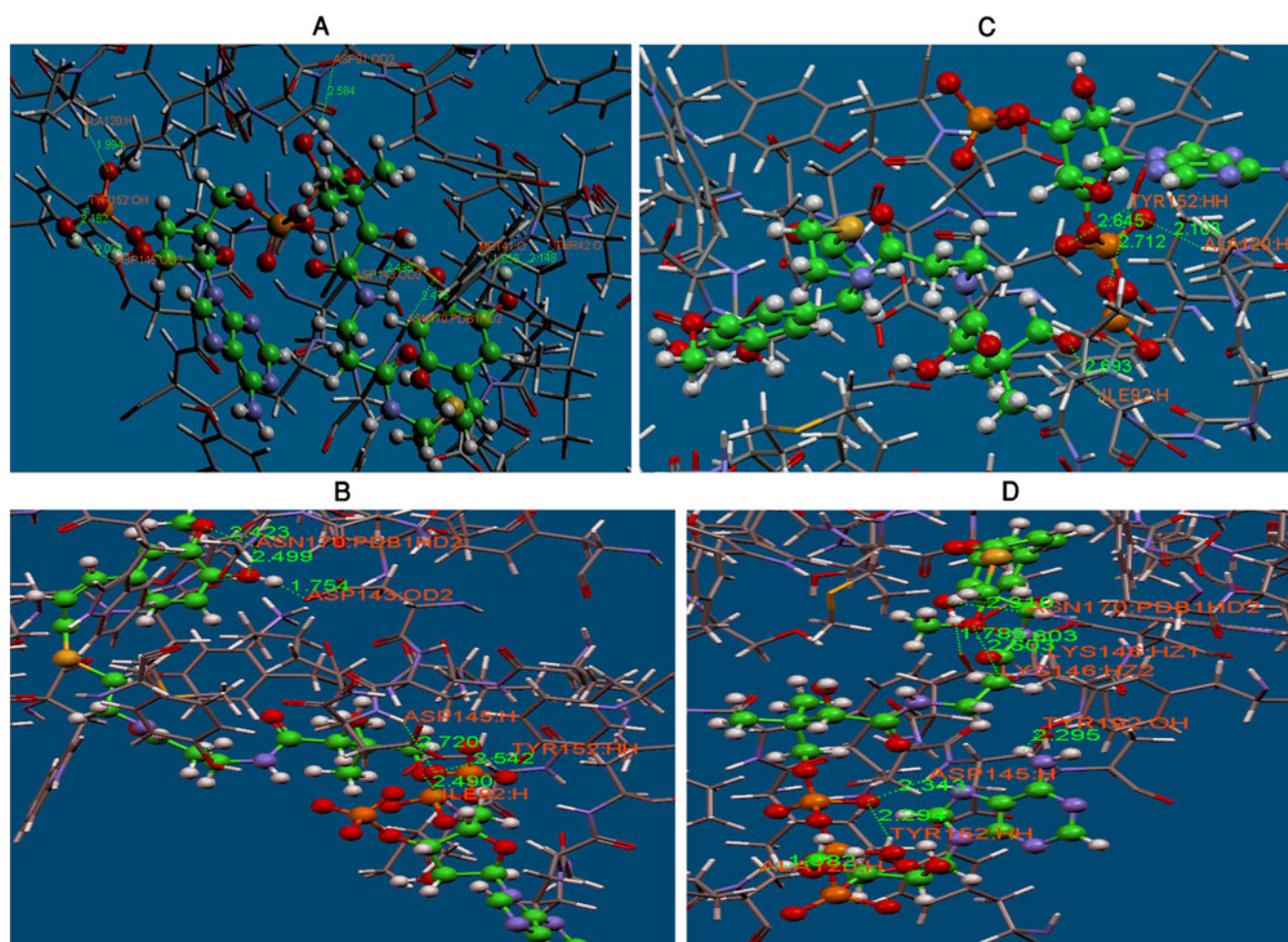


Fig. 5 Hydrogen bond interaction of caffeoyl CoA (a), feruloyl CoA (b), 5-hydroxyferuloyl CoA (c) and sinapoyl CoA (d) with active site residues of CCoAOMT1

appears that CCoAOMT1 and CCoAOMT2 and their templates 1SUS and 1SUI are well conserved in both sequence and structure, hence, their biological function may be identical. The comparison of active site residues of both CCoAOMT1 and 2 reveals that the active site is very much conserved with residues Lys1, Ser2, Leu3, Leu4, Tyr10, Ile13, Trp38, Ile40, Met41, Tht42, Thr43, Ser44, Asp46, Phe47, Ile66, Gly67, Val68, Tyr72, Ser73, Met90, Asp91, Ile92, Gly118, Ala120, Phe141, Asp143, Ala144, Asp145, Lys146, Tyr152, Asp169, Asn170, Trp173, Asn174, Tyr188, Tyr192, Val216, Gly217, Asp218. Therefore, these results are used to guide the protein-ligand docking experiments.

Molecular docking analysis of CCoAOMT1 and 2 with substrates

Hydrogen bond interactions

Docking studies of CCoAOMT isoforms indicates that hydrogen bond interactions of CCoAOMT2 with substrates

and products have much more affinity than CCoAOMT1. The detailed hydrogen bond interactions of CCoAOMT1 with caffeoyl CoA (Fig. 5a), feruloyl CoA (Fig. 5b), 5-hydroxyferuloyl CoA (Fig. 5c), and sinapoyl CoA (Fig. 5d); and of CCoAOMT2 with caffeoyl CoA (Fig. 6a), feruloyl CoA (Fig. 6b), 5-hydroxy feruloyl CoA (Fig. 6c), and sinapoyl CoA (Fig. 6d) are represented in their respective mentioned figures while the Gold Score with CCoAOMT1 and CCoAOMT2 are recorded respectively in Tables 4 and 5. The Gold Score of all interactions reveals that CCoAOMT1, among all its substrates and products, exhibits the highest binding affinity of 75.1856 with sinapoyl CoA, followed by 5-hydroxyferuloyl CoA, feruloyl CoA and caffeoyl CoA. Sinapoyl CoA forms 6 hydrogen bonds with ALA120:H, ASP145:H, LYS146:HZ1, LYS146:HZ2, TYR152:HH, ASN170:HD2. The CCoAOMT2 active site, among all its substrates and products, exhibits the highest binding affinity of 110.1452 with feruloyl CoA, followed by 5-hydroxyferuloyl CoA, sinapoyl CoA and caffeoyl CoA. The affinity of CCoAOMT2 with Feruloyl CoA which forms 5 hydrogen bonds with residues ILE92:H, ASP143:O, LYS146:H, LYS146:HZ3, ASN170:2HD2; is also highest

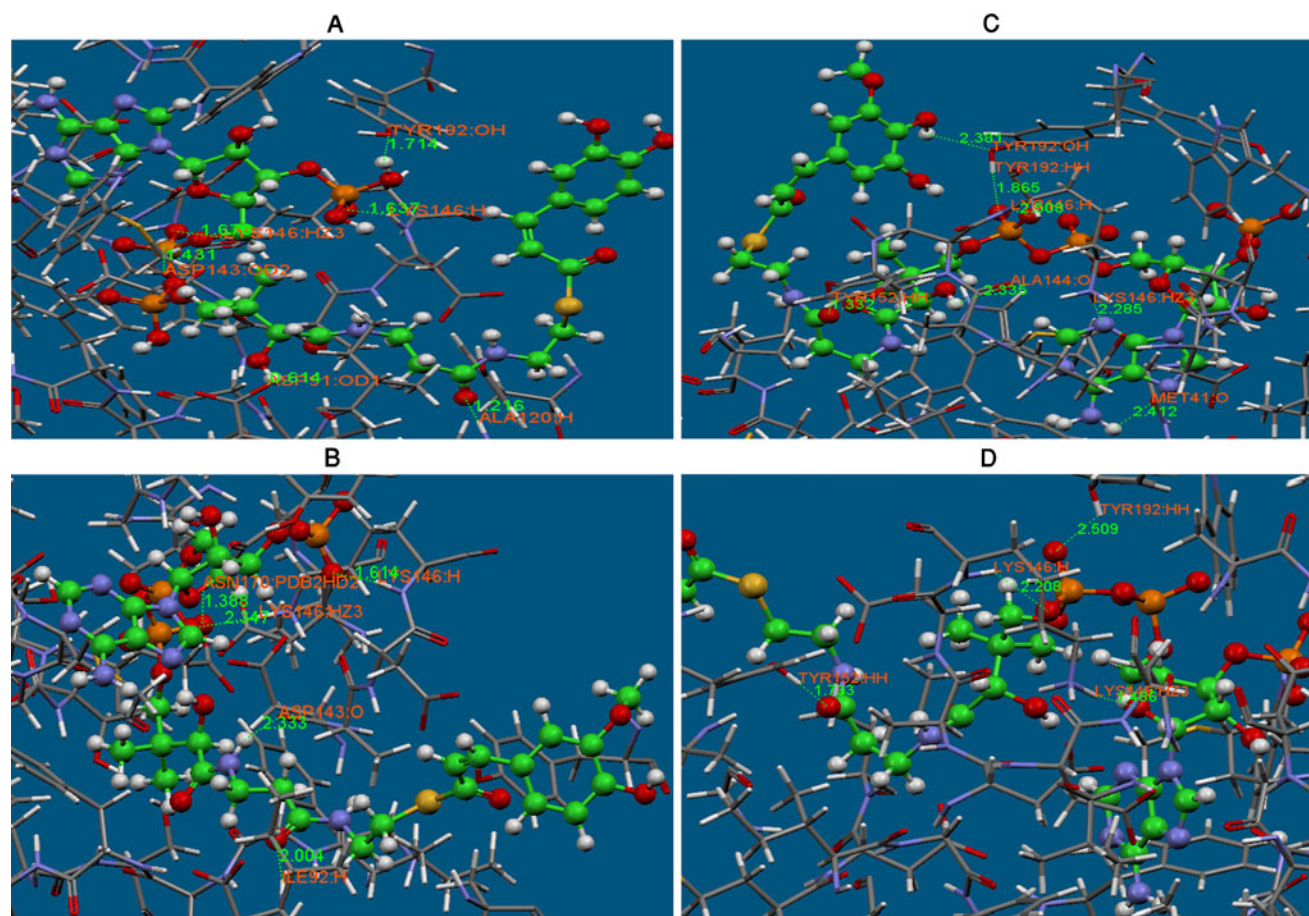


Fig. 6 Hydrogen bond interaction of caffeoyl CoA (a), feruloyl CoA (b), 5-hydroxyferuloyl CoA (c) and sinapoyl CoA (d) with active site residues of CCoAOMT2

Table 4 Hydrogen bond interactions with active site residues of CCOAOMT1

Substrate	Protein residue atoms participating in hydrogen bonding	Gold Score
Caffeoyl CoA	MET41:O THR42:O ASP91:OD2 ALA120:H ASP143:OD2 ASP145:OD2 TYR152:OH ASN170:1HD2	67.6098
Feruloyl CoA	ILE92:H ASP143:OD2 ASP145:H TYR152:HH ASN170:1HD2	69.5752
5-hydroxyferuloyl CoA	ILE92:H ALA120:H TYR152:HH	72.2044
Sinapoyl CoA	ALA120:H ASP145:H LYS146:HZ1 LYS146:HZ2 TYR152:HH ASN170:HD2	75.1856

Table 5 Hydrogen bond interactions with active site residues of CCOAOMT2

Substrate	Protein Atom Participating in Hydrogen Bonding	Gold Score
Caffeoyl CoA	ASP91:OD1 ALA120:H ASP143:OD2 LYS146:H LYS146:HZ3 TYR192:H	95.0714
Feruloyl CoA	ILE92:H ASP143:O LYS146:H LYS146:HZ3 ASN170:2HD2	110.1452
5-hydroxyferuloyl CoA	MET41:O ALA144:O LYS146:H LYS146:HZ3 TYR152:HH TYR192:HH TYR192:OH	101.4282
Sinapoyl CoA	LYS146:H LYS146:HZ3 TYR152:HH TYR192:HH	97.1207

among all the affinities exhibited by CCoAOMT isoforms with their substrates and products.

Discussion

Plant Caffeoyl CoA-*O*-methyltransferases (CCoAOMTs), belonging to class-I plant OMTs [1], plays a prime role in the synthesis of guaiacyl lignin and is essential in providing substrates for the synthesis of syringyl lignin. It also plays a pivotal role in the methylation of thioesters including methylation of 3-hydroxyl group of caffeoyl CoA, and CCoAOMT-mediated methylation reactions are vital to channel substrates for 5-methoxylation of hydroxycinnamates [1, 40]. The studies indicate that suppression of CCoAOMT enzyme in transgenic tobacco caused a decrease in lignin content, exhibiting the association of CCoAOMT with lignification [41]. However, in many plants CCoAOMT exist in two or more isoforms but it is not known whether the genes are expressed in a tissue specific manner or not and their functional redundancy. The variation analysis of both the isoforms indicates the existence of 13 amino acids differences which may be responsible for the difference in enzyme substrate interactions of CCoAOMT1 and CCoAOMT2, where CCoAOMT2 exhibits stronger interactions with substrates and products. To understand the structural and functional characteristics, the 3D structures of CCoAOMT1 and CCoAOMT2 of *Populus trichopora* were built by homology modeling, which revealed their possible interactions with substrates and products. CCoAOMT2 model with 96% residues falling in the most favorable regions of Ramachandran plot, is a more favorable conformation than CCoAOMT1 model, where only 92.4% residues fall in the most favorable region (Fig. 2) and the quality factor value of 98.174 is the same for both the isoforms (Fig. 3). The mean residue volume of isoforms 1 and 2 is 137.1 Å³ and 136.9 Å³, respectively. The active site residues are present in Rossman fold domain in models of both isoforms, where helices surrounded the β sheets are present in the center. The 3D structures of CCoAOMT1 and 2 isoforms show specific interactions of key amino acid residues in the active site with the substrates caffeoyl CoA, 5-hydroxyferuloyl CoA and products feruloyl CoA, sinapoyl CoA. These interactions are consistent with all of the previously reported experimental data concerning the catalytic activity of CCoAOMT1 and CCoAOMT2. Our models demonstrate the substrate-binding active site residues of the enzymes, which were not reported previously. Residues MET41, THR42, ASP91, ILE92, ALA120, ASP143, ASP145, LYS146, TYR152 and ASN170 of CCoAOMT1, are participating in the enzyme – substrate and product interaction and residues MET41, ASP91, ILE92, ALA120, ASP143, LYS146, TYR152, ASN170 and TYR192 of

CCoAOMT2, are participating in the enzyme – substrate and product interaction by forming hydrogen bonds with substrates and products. As already known, the hydrogen bonds play a very important role in maintenance of the enzymatic structure and catalytic activity of enzymes. The docking results indicated that CCoAOMT2, having highest affinity with feruloyl CoA which is also highest among all the affinities exhibited by both CCoAOMT isoforms with their substrates and products, binds with much higher affinity with all the substrates and products than CCoAOMT1 which has highest affinity for sinapoyl CoA. The results reveal that CCoAOMT2 is the active conformation that exists in *Populus trichopora* and it supports the work done by Nataraj, 2009, who stated the CCoAOMT2 as the active conformation in subabul plant [4]. All the informations of CCoAOMT and substrates interaction, concluded from results are beneficial for the mechanism study of CCoAOMT enzymatic reactions in *Populus trichopora*. The approach will be applicable for engineering regioselectivity of already existing enzymatic reactions, predictions of substrates and engineering 3D structures of enzymes, also for catalytic site study and docking analysis for enzyme substrate interactions of other enzymes.

Acknowledgments Research in VV's laboratory is supported by XI OBC plan grant of University of Hyderabad. The authors wish to thank Dr. S. C. Ghadi for providing computational facility, Prof. U.M. X. Sangodkar for his valuable suggestions. We also thank Dr. P.V. Bramhachari for helpful discussion.

References

- Park SH, Kim BG, Lee SH, Lim Y, Cheong Y, Ahn JH (2007) Molecular modeling and site directed mutagenesis of the O-methyltransferase, SOMT-9 Reveal amino acids important for its reaction and regioselectivity. Bull Korean Chem Soc 28:2248–2252
- Ibrahim RK, Bruneau A, Bantignies B (1998) Plant O-methyltransferases: molecular analysis, common signature and classification. Plant Mol Biol 36:1–10
- Joshi CP, Chiang VL (1998) Conserved sequence motifs in plant S-adenosyl-L-methionine dependent methyltransferases. Plant Mol Biol 37:663–674
- Pagadala NS, Arha M, Reddy PS, Kumar R, Sirisha VL, Prashant S, Reddy KJ K, Khan B, Rawal SK, Kishor PBK (2009) Phylogenetic analysis, homology modelling, molecular dynamics and docking studies of caffeoyl-CoA-O-methyl transferase (CCoAOMT 1 and 2) isoforms isolated from subabul (*Leucaena leucocephala*). J Mol Model 15:203–221
- Ferrer J, Zubieta C, Dixon RA, Noel JP (2005) Crystal structures of Alfalfa caffeoyl coenzyme A 3-O-Methyltransferase. Plant Physiol 137:1009–1017
- Parvathi K, Chen F, Guo D, Blount JW, Dixon RA (2001) Substrate preferences of O-methyltransferases in alfalfa suggest new pathways for 3-O-methylation of monolignols. Plant J 25:193–202
- Vance CP, Kirk TK, Sherwood RT (1980) Lignification as a mechanism of disease resistance. Annu Rev Phytopathol 18:259–288
- Lee JY, Lee S, Kim Y (2007) 3D structure of Bacillus halodurans O-methyltransferase, a novel bacterial O-methyltransferase by

- comparative homology modelling. Bull Korean Chem Soc 28:941–946
9. Lee YJ, Kim BG, Chong Y, Lim Y, Ahn JH (2008) Cation dependent O-methyltransferases from rice. *Planta* 227:641–647
 10. Ibdah M, Zhang XH, Schmidt J, Vogt T (2003) A novel Mg²⁺-dependent O-methyltransferase in the phenylpropanoid metabolism of *Mesembryanthemum crystallinum*. *J Biol Chem* 278:43961–43972
 11. Kim BG, Shin KH, Lee Y, Hur HG, Lim Y, Ahn JH (2005) Multiple regiospecific methylations of a flavonoid by plant O-methyltransferases expressed in *E. coli*. *Biotechnol Lett* 27:1861–1864
 12. Kim BG, Lee Y, Hur HG, Lim Y, Ahn JH (2006) Flavonoid 3'-O-methyltransferase from rice: cDNA cloning, characterization and functional expression. *Phytochemistry* 67:387–394
 13. Kim BG, Lee Y, Hur HG, Lim Y, Ahn JH (2006) Production of three O-methylated esculetins with *Escherichia coli* expressing O-methyltransferase from poplar [*Populus deltoides*]. *Biosci Biotechnol Biochem* 70:1269–1272
 14. Kim JH, Kim BG, Park Y, Han JH, Lim Y, Ahn JH (2006) Production of 5, 7-dihydroxy, 3-, 4-, 5-trimethoxyXavone from 5, 7, 3-, 4-, 5-pentahydroxyXavone using two O-methyltransferases expressed in *Escherichia coli*. *Agric Chem Biotechnol* 49:114–116
 15. Meyermans H, Morrell K, Lapierre C, Pollet B, De Bruyn A, Busson R, Herdewijn P, Devresse B, Van Beeumen J, Marita JM et al. (2000) Modifications in lignin and accumulation of phenolic glycosides in poplar xylem upon down-regulation of caffeoyl coenzyme A O-methyltransferase, an enzyme involved in lignin biosynthesis. *J Biol Chem* 275:36899–36909
 16. Li L, Osakabe Y, Chandrashekar PJ, Chiang VL (1999) Secondary xylemspecific expression of caffeoyl-coenzyme A 3-O-Methyltransferase plays an important role in the methylation pathway associated with lignin biosynthesis in loblolly pine. *Plant Mol Biol* 40:555–565
 17. Martz F, Maury S, Pincon G, Legrand M (1998) cDNA cloning, substrate specificity and expression study of tobacco caffeoyl-CoA 3-O-methyltransferase, a lignin biosynthetic enzyme. *Plant Mol Biol* 36:427–437
 18. Inoue K, Sewalt VJH, Balance GM, Ni W, Stürzer C, Dixon RA (1998) Developmental expression and substrate specificities of alfalfa caffeic acid 3-O-methyltransferase and caffeoyl coenzyme A 3-O-methyltransferase in relation to lignifications. *Plant Physiol* 117:761–770
 19. Ye ZH, Kneusel RE, Matern U, Varner JE (1994) An alternative methylation pathway in lignin biosynthesis in *Zinnia*. *Plant Cell* 6:1427–1439
 20. Kühnl T, Koch U, Heller W, Wellmann E (1989) Elicitor induced S-adenosyl-1-methionine:caffeoyl-CoA 3-O-methyltransferase from carrot cell suspension cultures. *Plant Sci* 60:21–25
 21. Pakusch AE, Kneusel RE, Matern U (1989) S-Adenosyl-1-methionine:trans-caffeoyl-coenzyme A 3-O-methyltransferase from elicitor-treated parsley cell suspension cultures. *Arch Biochem Biophys* 271:488–494
 22. Ye ZH (1997) Association of caffeoyl coenzyme expression with lignifying tissues A 3-O-Methyltransferase in several dicot plants. *Plant Physiol* 115:1341–1350
 23. Hoffmann L, Maury S, Bergdoll M, Thion L, Erard M, Legrand M (2001) Identification of the enzymatic active site of tobacco caffeoylcoenzyme A O-Methyltransferase by site-directed mutagenesis. *J Biol Chem* 276:36831–36838
 24. Maury S, Geoffroy P, Legrand M (1999) Tobacco O-Methyltransferases involved in phenylpropanoid metabolism. The different caffeoyl-coenzyme A/5-Hydroxyferuloyl-Coenzyme A 3/5-O-Methyltransferase and Caffeic Acid/5-Hydroxyferulic Acid 3/5-O-Methyltransferase classes have distinct substrate specificities and expression patterns. *Plant Physiol* 121:215–224
 25. Vidgren J, Svensson LA, Liljas A (1994) Crystal structure of catechol O-methyltransferase. *Nature* 368:354–357
 26. Zubieta C, He X-Z, Dixon RA, Noel JP (2001) Structures of two natural product methyltransferases reveal the basis for substrate specificity in plant O-methyltransferases. *Nat Struct Biol* 8:271–279
 27. Zubieta C, Kota P, Ferrer J-L, Dixon RA, Noel JP (2002) Structural basis for the modulation of lignin monomer methylation by caffeic acid/ 5-hydroxyferulic acid 3/5-O-methyltransferase. *Plant Cell* 14:1265–1277
 28. Sali A, Blundell TL (1993) Comparative protein modelling by satisfaction of spatial restraints. *J Mol Biol* 234:779–815
 29. Eswar N, Marti-Renom MA, Webb B, Madhusudhan MS, Eramian D, Shen M, Pieper U, Sali A (2006) Comparative protein structure modeling with MODELLER. *Current protocols in bioinformatics*. Wiley, New York, Supplement 15, 5.6.1-5.6.30
 30. Laskowski RA, MacArthur MW, Moss DS, Thornton JM (1993) PROCHECK: a program to check the stereochemical quality of protein structures. *J Appl Crystallogr* 26:283–291
 31. Colovos C, Yeates TO (1993) Verification of protein structures: patterns of nonbonded atomic interactions. *Protein Sci* 2:1511–1519
 32. Pedretti A, Villa L, Vistoli G (2004) VEGA - An open platform to develop chemo-bio-informatics applications, using plug-in architecture and script" programming". *J Comput Aided Mater Des* 18:167–173
 33. Phillips JC, Braun R, Wang W, Gumbart J, Tajkhorshid E, Villa E, Chipot C, Skeel RD, Kale L, Schulten K (2005) Scalable molecular dynamics with NAMD. *J Comput Chem* 26:1781–1802
 34. MacKerell AD, Brooks B, Brooks CL, Nilsson L, Roux B, Won Y, Karplus M (1998) CHARMM: the energy function and its parameterization with an overview of the program. In: Schleyer PVR et al. (eds) *The encyclopedia of computational chemistry* 1. Wiley, Chichester, pp 271–277
 35. MacKerell AD et al. (1998) All-atom empirical potential for molecular modeling and dynamics studies of proteins. *J Phys Chem B* 102:3586–3616
 36. Willard L, Ranjan A, Zhang H, Monzavi H, Boyko RF, Sykes BD, Wishart DS (2003) VADAR: a web server for quantitative evaluation of protein structure quality. *Nucleic Acids Res* 31(13):3316–3319
 37. Dundas J, Ouyang Z, Tseng J, Binkowski A, Turpaz Y, Liang J (2006) CASTp: Computed atlas of surface topography of proteins with structural and topographical mapping of functionally annotated residues. *Nucleic Acids Res* 34:W116–118
 38. Wheeler DL, Barrett T, Benson DA, Wheeler DL, Barrett T, Benson DA, Bryant SH, Canese K, Chetvermin V, Church DM et al. (2006) Database resources of the National Center for Biotechnology Information. *Nucleic Acids Res* 34:D173–180
 39. Jones G, Willett P, Glen RC (1995) Molecular recognition of receptor sites using a genetic algorithm with a description of desolvation. *J Mol Biol* 245:43–53
 40. Zhong R, Morrison WH, Himmelsbach DS, Poole FL, Ye ZH (2000) Essential role of caffeoyl coenzyme A O-methyltransferase in lignin biosynthesis in woody poplar plants. *Plant Physiol* 124:563–577
 41. Zhong R, Morrison WH, Negrel J, Ye ZH (1998) Dual methylation pathways in lignin Biosynthesis. *Plant Cell* 10:2033–2045